

# SOME PROBLEMS WITH THE METHOD OF FUNDAMENTAL SOLUTION USING RADIAL BASIS FUNCTIONS

Wang Hui

*(Department of Mechanics, Tianjin University, Tianjin 300072, China)*

Qin Qinghua

*(Department of Engineering, Australian National University, Canberra, ACT 0200, Australia)*

Received 23 March 2006; revision received 28 November 2006

**ABSTRACT** The present work describes the application of the method of fundamental solutions (MFS) along with the analog equation method (AEM) and radial basis function (RBF) approximation for solving the 2D isotropic and anisotropic Helmholtz problems with different wave numbers. The AEM is used to convert the original governing equation into the classical Poisson's equation, and the MFS and RBF approximations are used to derive the homogeneous and particular solutions, respectively. Finally, the satisfaction of the solution consisting of the homogeneous and particular parts to the related governing equation and boundary conditions can produce a system of linear equations, which can be solved with the singular value decomposition (SVD) technique. In the computation, such crucial factors related to the MFS-RBF as the location of the virtual boundary, the differential and integrating strategies, and the variation of shape parameters in multi-quadric (MQ) are fully analyzed to provide useful reference.

**KEY WORDS** meshless method, analog equation method, method of fundamental solution, radial basis function, singular value decomposition, Helmholtz equation

## I. INTRODUCTION

Since the method of fundamental solution (MFS) was first developed in 1964<sup>[1]</sup>, the MFS has become a standard extensively used in science and engineering<sup>[2-5]</sup>. Owing to the introduction of fictitious sources outside the domain, singular and near singular integrals are completely prevented. In addition, the MFS has the advantages of rapid convergence<sup>[6,7]</sup>, high accuracy, simple theory and convenience of implementation by programming. However, there are several inherent drawbacks with this method. The first is the location of the fictitious source points. So far, no final justification for determining their locations has yet been found. The second drawback is that it is difficult to deal with non-homogeneous problems with MFS. The domain integrals required in non-homogeneous problems make the MFS inconvenient and less advantageous. The third disadvantage is that the MFS is strongly dependent on the fundamental solutions for the problem under consideration which, however, are hard to obtain in complicated cases. Fortunately, in recent years, the MFS has been provided with new potentials by the radial basis functions (RBFs)<sup>[8-10]</sup> and the analog equation method (AEM)<sup>[11]</sup>. The RBF can be used to approximate the non-homogeneous part and the MFS is dedicated to finding the homogeneous part. Although the second obstacle is overcome, the use of RBF brings new problems, such as the

choice of RBF's and the interpolating points scheme being an important one. At present, some widely supported RBF's (GS-RBF) such as power spline (PS), thin plane spline (TPS), multi-quadric (MQ) and Gaussian (GS) are frequently used in computation<sup>[9,10]</sup>. The PS and TPS are piecewise smooth, while MQ and GS are infinitely smooth. They work well in many cases and it is pointed out that, for the MQ and GS, their shape parameters should be carefully selected to reach the best accuracy and stability. Next, the RBF approximation depends on the interpolation points, which can be located either in the domain or on the boundary. Generally, the RBF approximation is related to the governing equation and independent of the boundary conditions. So, the internal interpolation points usually are selected during computation. For example, for the famous Kansa's method<sup>[15]</sup>, when the interpolation points include boundary points, the results may become unstable. However, whether the interpolation points can include the boundary points in the MFS with RBF interpolation (MFS-RBF) is still an interesting problem worth further investigation. The AEM is another effective tool for converting the original governing equation into the equivalent Poisson's equation, so that the fundamental solution of the Laplacian operator can be used instead of the original governing equation.

In the present paper, our purpose it is to thoroughly study the influence factors on the proper use of the MFS-RBF by solving the Helmholtz problem. This paper is arranged as follows. In §II, the problems under consideration are depicted. In §3.1, the AEM is used to convert the original governing equation into a standard Poisson's equation, and next, in §3.2 and §3.3, the particular and homogeneous solutions are derived in terms of RBF approximation and the MFS, respectively. Consequently, a composite solution is obtained in §3.4. By making the composite solution obtained satisfy the boundary conditions at the boundary nodes and the governing equation at the interpolation points all unknowns can be determined. In §3.5, some influence factors related to the MFS-RBF are gathered, which will be investigated with illustrative examples given in §IV. Finally, In §V, relevant conclusions are drawn about the meshless method.

## II. THE HELMHOLTZ PROBLEMS

Consider the general potential problem as follows:

$$\sum_{i=1}^d \sum_{j=1}^d k_{ij} \frac{\partial^2 u}{\partial x_i \partial x_j} + \lambda^2 u = f(X), \quad X \in \Omega \quad (1)$$

with boundary conditions

$$u(X) = \bar{u}, \quad X \in \Gamma_u; \quad \frac{\partial u(X)}{\partial n} = \bar{q}, \quad X \in \Gamma_q \quad (2)$$

where  $k_{ij}$  is the material property and  $\lambda$  is the wave number.  $f(X)$  is a known forcing source function, and  $n$  is the unit outward normal.  $X \in R^d$ ,  $d$  is the dimension of domain  $\Omega$ , which has a piecewise smooth boundary  $\Gamma = \Gamma_u + \Gamma_q$ .  $\bar{u}$  and  $\bar{q}$  are specified values on the boundary, respectively.

## III. APPLICATION OF THE MFS-RBF MESHLESS METHOD

### 3.1. The Analog Equation Method (AEM)<sup>[11]</sup>

First, we assume that  $u = u(X)$  is the sought-for solution to the boundary value problem (BVP) consisting of Eqs.(1) and (2a)-(2b). According to the concept of the analog equation, if the standard Laplace operator is applied to this solution, we have

$$\nabla^2 u(X) = b(X), \quad X \in \Omega \quad (3)$$

where  $b(X)$  is the unknown fictitious source induced.

It is evident that the solution  $u(X)$  in the linear differential equation (3) can be split into a homogeneous part  $u_h$  and a particular part  $u_p$ , such that

$$u = u_h + u_p \quad (4)$$

where the particular solution  $u_p$  satisfies the equation

$$\nabla^2 u_p = b(X), \quad X \in \Omega \quad (5)$$

but is not required to satisfy any boundary conditions, and the related homogeneous solution  $u_h$  satisfies

$$\begin{aligned}\nabla^2 u_h(X) &= 0, & X \in \Omega \\ u_h(X) &= \bar{u} - u_p(X), & X \in \Gamma_u \\ q_h(X) &= \bar{q} - q_p(X), & X \in \Gamma_q\end{aligned}\quad (6)$$

### 3.2. RBF Interpolation for the Particular Solution

In this process, our purpose it is to derive the particular solution. The dual reciprocity method (DRM)<sup>[12,13]</sup> with RBFs in BEM is a promising approach to this task. First,  $b(X)$  in Eq.(3) is approximated by

$$b(X) = \sum_{i=1}^M \alpha_i \phi_i(X) \quad (7)$$

where  $M$  is the number of interpolating points probably including the internal and boundary collocation points;  $\alpha_i$  are coefficients to be determined, and  $\phi_i$  is a set of RBF's. Whether the interpolating points can include the boundary points is confusing and will be investigated later.

Similarly, the particular solution  $u_p$  is also approximated by means of the same coefficients

$$u_p(X) = \sum_{i=1}^M \alpha_i \Phi_i(X) \quad (8)$$

where  $\Phi_i$  is the corresponding set of approximate particular solutions. As the particular solution  $u_p$  satisfies Eq.(5), the key to this approximation is that such a relation as

$$\nabla^2 \Phi_i(X) = \phi_i(X) \quad (9)$$

exists.

At present, there are two different strategies for obtaining the approximate particular solutions  $\Phi_i$  in terms of RBF's<sup>[14]</sup>. The standard one is that  $\phi_i$  in Eq.(9) is first selected, and then the related  $\Phi_i$  is derived by analytically integrating the given differential operator, which is a Laplacian operator here. This strategy is completely mathematically reliable, however, it should be pointed out that this approach strongly depends on the RBF selected and can be performed only for some simple operators. The other is a reverse process. We can choose  $\Phi_i$  as RBF's first and then derive the corresponding  $\phi_i$  through a simple differential process. This inverse treatment is in fact similar to the direct interpolation in the Kansa's method<sup>[15]</sup>. In this paper, the two strategies will be compared based on the infinite smoothing multi-quadric (MQ) and the related formulations are listed in Table 1.

Table 1. Integrating and differential strategies with MQ for 2D Laplace operator

	integrating strategy	differential strategy
$\phi$	$\sqrt{r^2 + c^2}$	$\frac{r^2 + 2c^2}{(\sqrt{r^2 + c^2})^3}$
$\Phi$	$-\frac{c^3 \ln(c\sqrt{r^2 + c^2} + c^2)}{3} + \frac{(r^2 + 4c^2)\sqrt{r^2 + c^2}}{9}$	$\sqrt{r^2 + c^2}$

Since the induced term  $b(X)$  is totally dependent on the unknown field  $u(X)$ , the coefficients  $\alpha_i$  cannot be directly determined by solving Eq.(7). Similarly, the particular solution  $u_p$  also cannot be determined in Eq.(8). Fortunately, in the MFS-RBF based on the AEM, our purpose it is to obtain the expression such as Eq.(8) instead of the specified values of the particular solution. This idea is also used to obtain the homogeneous solution, which will be derived with the MFS in the next section.

### 3.3. The MFS for the Homogeneous Solution

To obtain a strong solution of Laplace equation (6),  $N$  artificial source points  $Y_j \in R^d$  ( $j = 1, 2, \dots, N$ ) are arranged on the virtual boundary outside the domain (Fig.1). According to the basic definition of the fundamental solution for the Laplace operator,

$$\nabla^2 u^*(X, Y_j) = 0, \quad X \neq Y_j \quad (10)$$

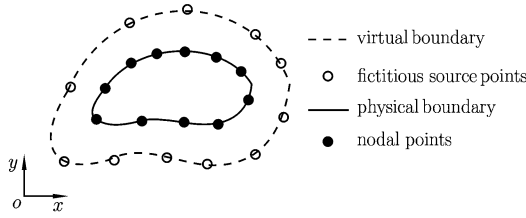


Fig. 1. Illustration of collocation points on the physical and virtual boundary.

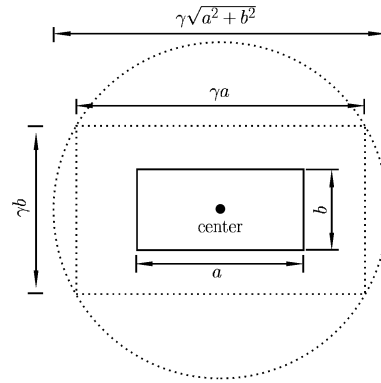


Fig. 2. Similar and circular virtual boundaries related to a simple rectangular domain.

the linear combination of them

$$u_h(X) = \sum_{j=1}^N \beta_j u^*(X, Y_j), \quad X \neq Y_j \tag{11}$$

should satisfy the Laplace equation (6). Where  $X$  is an arbitrary field point in the domain and  $u^*$  is the fundamental solution for the Laplacian operator given in  $R^2$

$$u^*(X, Y) = \frac{1}{2\pi} \ln \frac{1}{r(X, Y)} \tag{12}$$

Theoretically, the fictitious source points can be distributed randomly outside the domain, that is, the shape of the virtual boundary is arbitrary. However, in terms of computation, the circular and similar virtual boundaries are widely used to get the greatest convenience<sup>[3, 16]</sup>. For example, the shapes of a virtual boundary can be chosen to be either rectangular or circular for a rectangular domain (see Fig.2). In order to measure the location of the virtual boundaries, in our analysis, a real ratio parameter  $\gamma$  defined as

$$\gamma = \frac{\text{characteristic length of the virtual boundary}}{\text{characteristic length of the physical boundary}}$$

is introduced. For instance, for the rectangular domain shown in Fig.2, the geometries of the circular or rectangular virtual boundaries can be determined in terms of the ratio parameter  $\gamma$ , respectively.

### 3.4. The Final Composite Solution and Numerical Process

Based on the above process the final composite solution  $u(X)$  we are seeking for Eqs.(1) and (2) can be obtained

$$u(X) = \sum_{i=1}^M \alpha_i \Phi_i(X) + \sum_{j=1}^N \beta_j u^*(X, Y_j) \tag{13}$$

which has continuous differential of the second order.

Finally, in order to determine  $M + N$  unknowns  $\alpha_i$  and  $\beta_j$ , we can force Eq.(13) to satisfy the governing equation (1) at  $M$  interpolation points inside the domain  $\Omega$  or on its boundary and the specified boundary conditions (2) at  $N$  nodal points on the physical boundary. As a result, a set of  $M + N$  linear equations can be obtained, from which all unknowns can be solved. Furthermore, the solution  $u$  and its derivative at the arbitrary field point  $X$  can be calculated using Eq.(13).

### 3.5. Topics on the MFS-RBF

From the above process, it can be seen that there are several crucial factors that should be considered in the process of the MFS-RBF. For convenience, they are listed as follows:

- (a) The shape and location of the virtual boundary
- (b) Whether the interpolating points can include the boundary points

(c) The integrating and differential strategies for the use of RBFs

(d) Sensitivity to the shape parameter  $c$  in MQ

In this paper, these factors will be discussed by solving the 2D isotropic or anisotropic Helmholtz problems with different wave numbers in the simple and complicated domains in the next section.

#### IV. NUMERICAL EXAMPLES

In our computation, the circular virtual boundary is preferred, unless otherwise specified. In addition, the singular values decomposition (SVD) algorithm is employed to solve the linear system of equations. Generally, the coefficient matrix is singular if its condition number is infinite, and it is ill-conditioned if its condition number is too large, that is, if its reciprocal approaches the machine's floating-point precision. In order to properly use SVD, zeroing the small singular values is suggested<sup>[17]</sup>. Moreover, for the sake of convenience, only the Dirichlet boundary condition is involved and the uniformly distributed collocation scheme is used.

Finally, to measure the accuracy of the approximation, the average relative error  $\text{Arerr}(u)$  defined as

$$\text{Arerr}(u) = \sqrt{\frac{\sum_{j=1}^L (u_j - \tilde{u}_j)^2}{\sum_{j=1}^L (u_j)^2}} \quad (14)$$

is introduced, where  $u_j$  and  $\tilde{u}_j$  are the analytical and numerical results at the computing points of interest, respectively, and  $L$  is the total number of these points.

##### 4.1. 2D Isotropic Helmholtz Problem in a Unit Square Domain

Consider a 2D inhomogeneous Helmholtz equation given by

$$\nabla^2 u + \lambda^2 u = 2 \sin(\mu x) \cos(\mu y) + 4\mu x \cos(\mu x) \cos(\mu y) \quad (15)$$

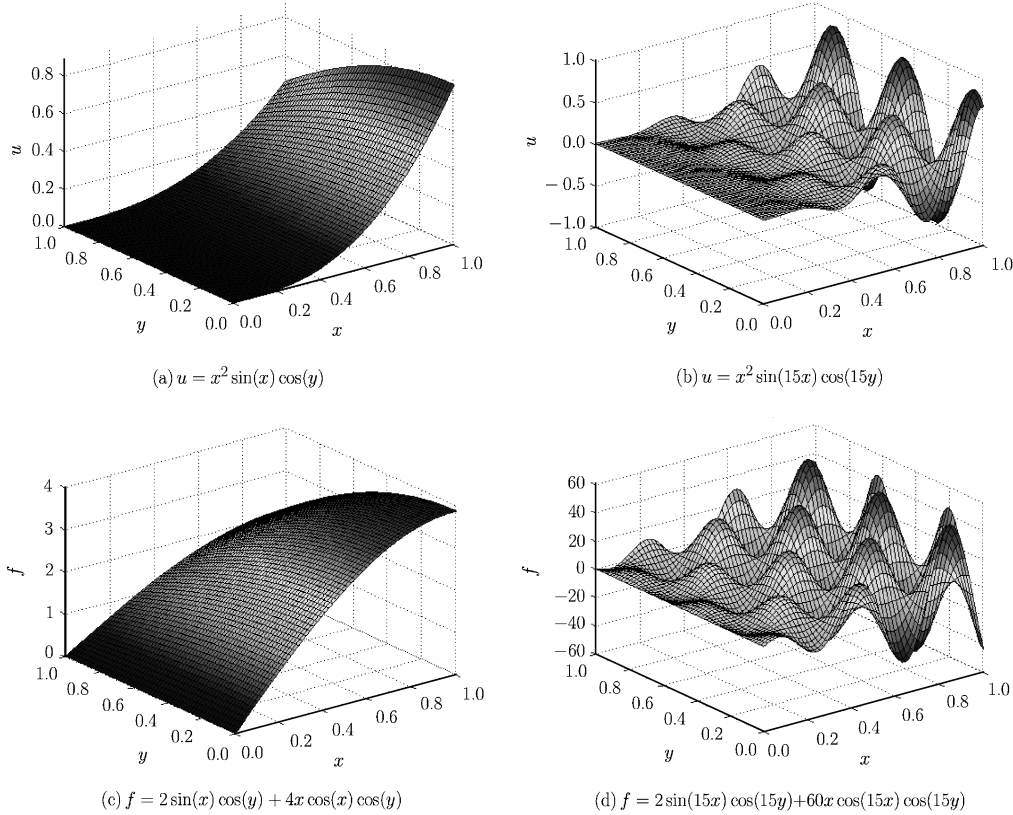


Fig. 3. Distributions of the accurate solution and the right-handed term with various parameters  $\mu$  in a unit square.

in a square domain. The boundary condition is applied by the particular function ( $\lambda = \mu\sqrt{2}$ )

$$u = x^2 \sin(\mu x) \cos(\mu y) \tag{16}$$

The distributions of the accurate solution and the right-handed term in a unit square domain with various parameters  $\mu$  are shown in Fig.3, from which we can see that the greater the variation of the function is, the larger  $\mu$  is.

In order to demonstrate the influence of the boundary interpolating points, we first compare the two interpolation schemes, i.e. the whole interior interpolating points scheme and the interior and boundary interpolating points scheme, with the results shown in Fig.4, from which we can see that the latter produces better results than the former. So, in the computation below, we select the internal and boundary points to carry out the RBF approximation, instead of all the internal points, which is different from the Kansa's method.

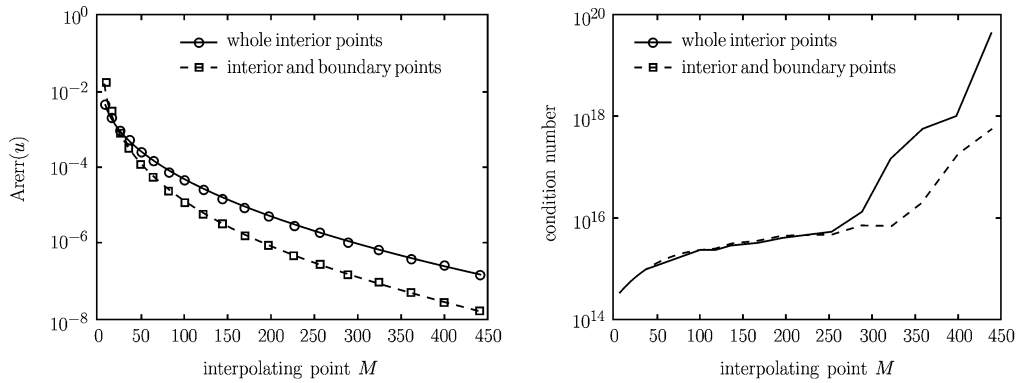


Fig. 4. Comparison between two schemes in the choice of the interpolating points with  $N=44$ ,  $c = 0.5$  and  $\gamma = 3.0$  for the case of  $\mu = 1$ .

Next, we shall test the influence of the location of the virtual boundary. When the circular virtual boundary is used, the error distribution is evaluated for the case of  $\mu = 1, 5, 10, 15$  and the results in Fig.5 show that the stable region of the parameter  $\gamma$  in which relatively stable and small errors occur decreases as the wave number increases. For example, for the case of  $\mu = 1$ , the ratio parameter  $\gamma$  in the range  $[1.4, 9]$  can produce relatively stable and small error distribution, while for the case of  $\mu = 5$ , the range changes to  $[1.4, 6]$ .

The effectiveness of MQ depends on the shape parameter  $c$ . Despite the use of the cross validation technique<sup>[9]</sup> to predict the good value of the shape parameter in solving the Poisson's problem, this

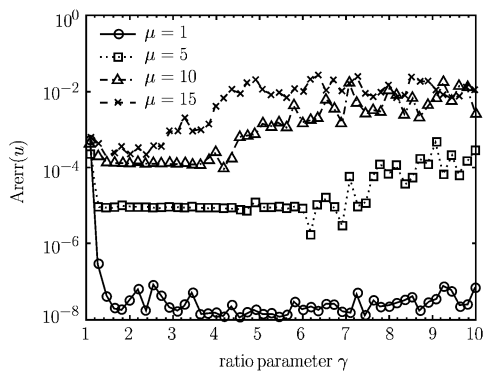


Fig. 5. Influences of the ratio parameter  $\gamma$  with  $N = 44$ ,  $M = 441$  and  $c = 0.5$ .

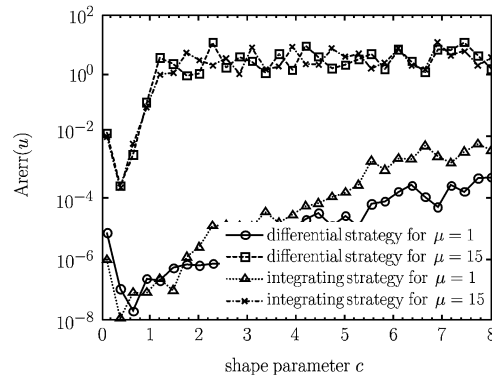
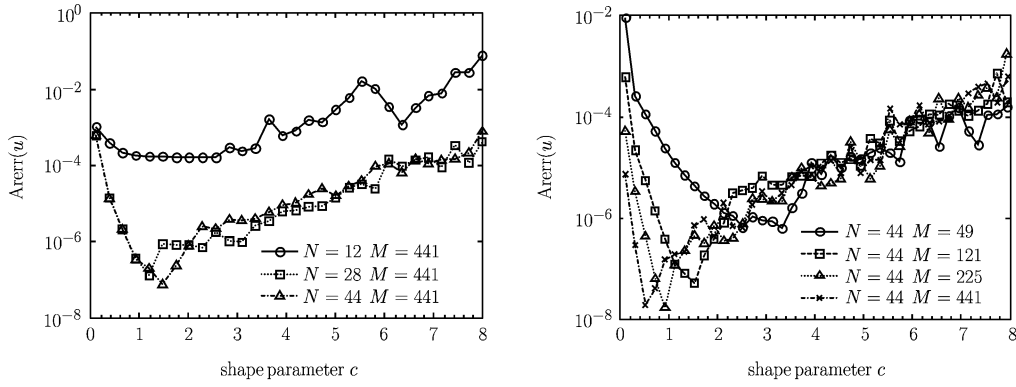
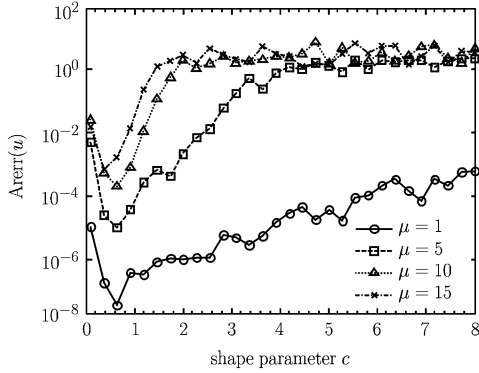
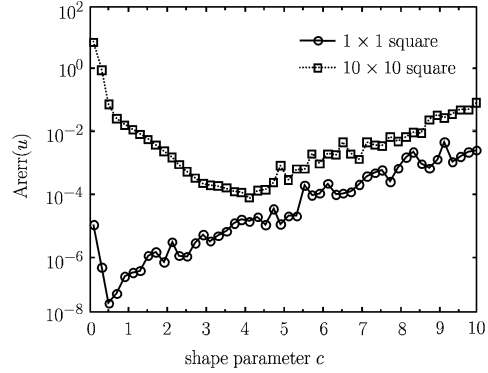


Fig. 6. Comparison of differential and integrating strategies with  $N = 44$ ,  $M = 441$  and  $\gamma = 3.0$ .


 Fig. 7. Influences of the shape parameter  $c$  on convergence with  $\gamma = 3.0$  for the case of  $\mu = 1$ .

approach can hardly be extended to the MFS-RBF employed in this paper. We shall now analyze the impact of the variation of the shape parameter numerically. First, a comparison should be made between the differential and integrating strategies in the process of the derivation of the approximate particular solution. It can be seen from Fig.6 that there is little difference in the good shape parameter between these two strategies, especially for the case of a high wave number. So, in the computation below, the simple differential strategy will be used to carry out numerical experiment. Secondly, the influence of the shape parameter on convergence is considered in Fig.7. It is apparent that the best value of  $c$  shifts with the variation of the number of boundary nodes or interpolating points, which is disadvantageous to maintaining the convergence. The influence of  $c$  with various wave numbers and the related results are shown in Fig.8, from which it can be seen that the best parameter  $c$  is basically independent of the variation of the wave number, once the collocation points are determined. Finally, the influence of the geometry of the domain on the shape parameter should be considered. The results in Fig.9 show that the geometry of the domain affects the best value of  $c$ . For the square domains of 1 by 1 and 10 by 10, the best values of  $c$  are close to 0.5 and 4.1, respectively.


 Fig. 8. Influences of the shape parameter  $c$  with  $N = 44$  and  $M = 441$ ,  $\gamma = 3.0$  for different wave numbers.

 Fig. 9. Influences of geometry on the shape parameter  $c$  with  $N = 44$  and  $M = 441$ ,  $\gamma = 3.0$  for the case of  $\mu = 1$ .

#### 4.2. 2D Anisotropic Helmholtz Problem in a Multi-domain

Let us consider a 2D anisotropic Helmholtz equation

$$\frac{\partial^2 u}{\partial x_1^2} + \frac{\partial^2 u}{\partial x_1 \partial x_2} + \frac{\partial^2 u}{\partial x_2^2} + \lambda^2 u = 0 \quad (17)$$

To illustrate the accuracy, the following analytical solution

$$u = \sin\left(\frac{\sqrt{3}}{2}\mu x\right) + \cos\left[\mu\left(y - \frac{x}{2}\right)\right] \quad (18)$$

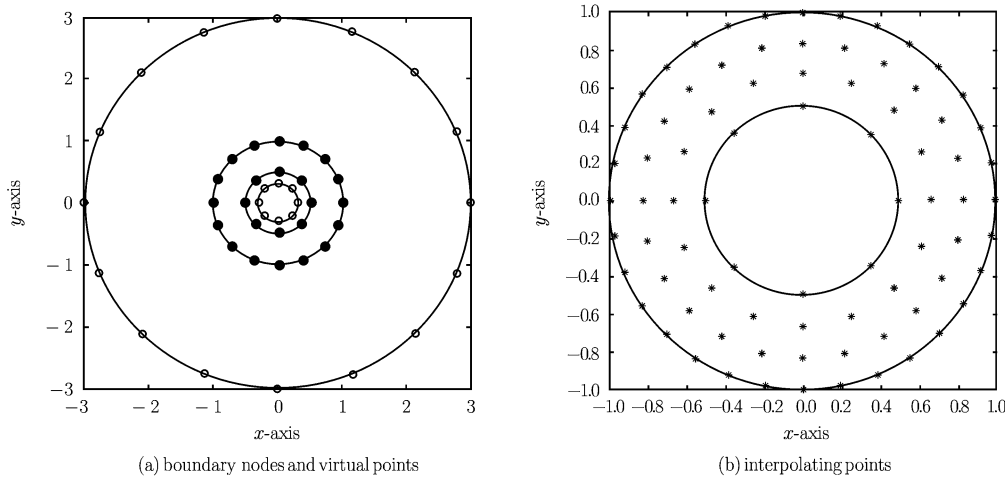


Fig. 10. Configurations of nodes, virtual source points and interpolating points.

with the relation of  $\lambda = \sqrt{3}\mu/2$  is tested in a multi-circular domain.

For this anisotropic problem in the multi-domain, attention focuses on the investigation of the locations of inner and outer virtual boundaries and the variation of the shape parameter of the same collocation points as  $N = 36, M = 168$ . Figure 11 shows the influence of the ratio parameters  $\gamma_{inner}$  and  $\gamma_{outer}$  corresponding to the inner and outer physical boundaries, respectively. It is clear that the smaller  $\gamma_{outer}$  is and the larger  $\gamma_{inner}$  is, the larger the error will be. This is mainly due to the singular interference of the fundamental solution when the virtual boundaries are close to the physical boundaries. In Fig.12, the influence of the shape parameter  $c$  is plotted for various wave numbers. We can see that the good value of the shape parameter approaches 1.7.

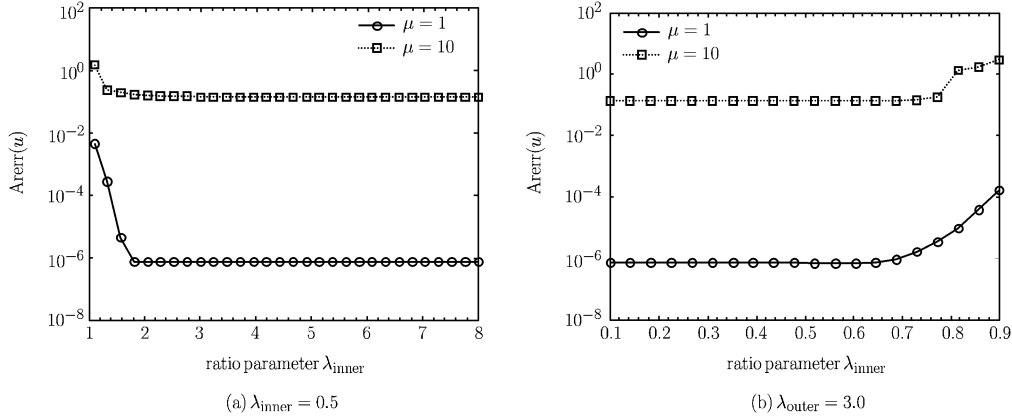


Fig. 11. Influences of the ratio parameter  $\gamma$  with  $N = 36, M = 168$  and  $c = 0.5$  for various wave numbers.

### V. CONCLUSIONS

The MFS-RBF coupled with the AEM is used to solve 2D isotropic and anisotropic Helmholtz problems. The influence factors in the process of this meshless method are investigated in detail. From the numerical demonstration, these factors influence one another and make it difficult to obtain general decisions, especially for the choice of the shape parameter in MQ. In summary, we can obtain the following conclusions:

- (a) The best location of the virtual boundary is influenced by the wave number.

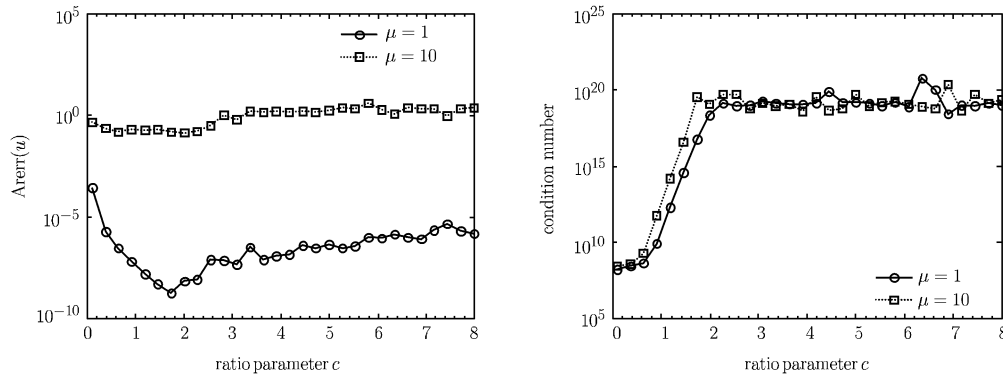


Fig. 12. Influences of the shape parameter  $c$  with  $N = 36$ ,  $M = 168$  and  $\gamma_{\text{inner}} = 0.5$ ,  $\gamma_{\text{outer}} = 3.0$  for various wave numbers.

(b) The choice of the shape parameter  $c$  affects the convergence, in other words, the collocation points affect the best value of the shape parameter.

(c) The geometries of the domain influence the shape parameter  $c$ .

(d) In the process of obtaining the approximate particular solution, the integrating and differential strategies are equally effective.

## References

- [1] Kupradze V.D. and Aleksidze M.A. The method of functional equations for the approximate solution of certain boundary value problems. *USSR Comput. Math. Math. Phys.*, 1964, 4: 82-126.
- [2] Golberg M.A. and Chen C.S. The method of fundamental solutions for potential, Helmholtz and diffusion problems. In: *Boundary Integral Methods-Numerical and Mathematical Aspects*, ed. Golberg M.A., Boston/Southampton: Computational Mechanics Publications, 1999: 105-176.
- [3] Fairweather G. and Karageorghis A. The method of fundamental solutions for elliptic boundary value problems. *Adv. Comput. Math.*, 1998, 9: 69-95.
- [4] Poullikkas A., Karageorghis A. and Georgiou G. The method of fundamental solutions for three-dimensional elastostatics problems. *Computers and Structures*, 2002, 80: 365-370.
- [5] Karageorghis A. The Method of fundamental solutions for the calculation of the eigenvalues of the Helmholtz equation. *Applied Mathematics Letters*, 2001, 14: 837-842.
- [6] Li Xin. On convergence of the method of fundamental solutions for solving the Dirichlet problem of Poisson's equation. *Advances in Computational Mathematics*, 2005, 23: 265-277.
- [7] Peter Mitic, Youssef F. Rashed. Convergence and stability of the method of meshless fundamental solutions using an array of randomly distributed sources. *Eng. Anal. Bound. Elem.*, 2004, 28: 143-153.
- [8] Golberg M.A., Chen C.S. and Bowman H. Some recent results and proposals for the use of radial basis functions in the BEM. *Eng. Anal. Bound. Elem.*, 1999, 23: 285-296.
- [9] Golberg M.A., Chen C.S. and Karur S.R. Improved multiquadric approximation for partial differential equations. *Eng. Anal. Bound. Elem.*, 1996, 18: 9-17.
- [10] Li J.C. Mathematical justification for RBF-MFS. *Eng. Anal. Bound. Elem.*, 2001, 25: 897-901.
- [11] Katsikadelis J. T. The analog equation method—a powerful BEM—based solution technique for solving linear and nonlinear engineering problems. In: Brebbia CA, ed., *Boundary Element Method XVI*, Southampton: CLM Publications, 1994: 167-182.
- [12] Patridge P.W., Brebbia C.A. and Wrobel L.W. *The Dual Reciprocity Boundary Element Method*. Computational Mechanics Publication, Southampton, 1992: 69-75.
- [13] Zou J, Li Z L et al. Boundary element method for model analysis of 2-D composite structure. *Acta Mechanica Solida Sinica*, 1998, 11: 63-71.
- [14] Chen W, Tanaka M. A meshless, integration-free and boundary-only RBF technique. *Computers & Mathematics with Applications*, 2002, 43: 379-391.
- [15] Kansa E.J. Multiquadrics: A scattered data approximation scheme with applications to computational fluid dynamics. *Comput. Math. Appl.*, 1990, 19: 147-161.
- [16] Sun H C, Zhang L Z, et al. *Nonsingularity Boundary Element Methods*. Dalian: Dalian University of Technology Press, 1999: 185-189.
- [17] William H. Press, Saul A. Teukolsky, et al. *Numerical recipes in C* (2nd ed. edition). Cambridge University Press, 2001: 59-70.